Journal of Water Process Engineering 59 (2024) 104959

Contents lists available at ScienceDirect

Journal of Water Process Engineering

journal homepage: www.elsevier.com/locate/jwpe

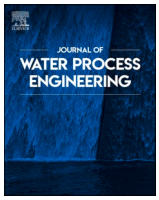

Field installation of ion exchange technology for purification of retention reservoirs from nitrogen-based nutrient contamination

Piotr Cyganowski [a,*,1], Łukasz Gruss [b,1], Witold Skorulski [c], Tomasz Kabat [c], Paweł Piszko [d], Dorota Jermakowicz-Bartkowiak [a], Krzysztof Pulikowski [b], Mirosław Wiatkowski [b]

[a] Department of Process Engineering and Technology of Polymer and Carbon Materials, Faculty of Chemistry, Wrocław University of Science and Technology, Wyb. S Wyspianskiego 27, 50-370 Wrocław, Poland
[b] Institute of Environmental Engineering, Wrocław University of Environmental and Life Sciences, pl. Grunwaldzki 24, 50-363 Wrocław, Poland
[c] Art Strefa Witold Skorulski, ul. Śniadeckich 45/6, 51-604 Wrocław, Poland
[d] Department of Polymer Engineering and Technology, Faculty of Chemistry, Wrocław University of Science and Technology, Wyb. S Wyspianskiego 27, 50-370 Wrocław, Poland

ARTICLE INFO

Editor: Jingming Duan

Keywords:
Fertiliser contamination
Anion exchange resin
Reservoir, surface water quality

ABSTRACT

N- and P-nutrient contamination is recognised as one of the key factors that reduces the quality of water. In this context, a new water purification installation was set up in the *Turawa* reservoir (district Opole, Poland). The process involves ion exchange columns operated in twin configuration: once one column filtrates water, the second one regenerates. The installation design is modular, and the devices are placed in a container station. This enables efficient water purification in various locations and further offers scalability. The research focused on the design and optimization of the installation, as well as environmental assessment of how the installation influenced the quality of water. This technology afforded a decrease in the concentrations of NO_3^- ions, suggesting an apparent selectivity. The removal of NO_3^- reached 97 % and was maintained for over 100 m^3 of purified water. In turn, the removal of PO_4^{3-} was not effective; however, the collected data allowed the installation design to be adjusted such that the cascade arrangement of ion exchange columns can be considered. The technology was assessed over all four seasons in the two-year test period (2020−2021). This revealed that environmental factors, such as season, air temperature, wind, and relative humidity, influence the operation of the installation. The installation functions optimally in spring with an average air temperature of 11–20 °C, high relative humidity of 90–100 %, and an average wind speed of 2 m/ s. The implementation of the technique could easily broaden the perspectives of Earth's water preservation and sustainability.

1. Introduction

The environmental burden arising from the excessive use of fertilisers and nutrient contamination is acknowledged by the United States Environmental Protection Agency (EPA) and the European Union (EU) as a part of the major challenges of water preservation and sustainability [58–61]. Preservation and purification of retention reservoirs and lakes are potential solutions to these challenges. These can be implemented using flood management plans [1], and are recognised as key tools for maintaining and increasing freshwater resources [2,3]. Unfortunately,

Abbreviations: PO, charge pump; FL, mechanical filter; F2, ion exchange column 1; F3, ion exchange column 2; ZZR, regenerant container; ZP, effluent container; S1, season 1, spring; S2, season 2, summer; S3, season 3, autumn; S4, season 4, winter; TKN, total Kjeldahl nitrogen; ON, organic nitrogen; TN, total nitrogen; TP, total phosphorus; DO, dissolved oxygen; BOD_5, five-day biochemical oxygen demand; COD_{Mn}, chemical oxygen demand (permanganate index); TSS, total suspended solids; TDS, dissolved substances; EC, electrical conductivity; ATR-FTIR, attenuated total reflectance Fourier transform infrared spectroscopy; SEM, scanning electron microscopy; EDX, energy dispersive X-ray analyser; AT_L, low air temperature (0–10 °C); AT_M, medium air temperature (11–20 °C); AT_H, high air temperature (21–30 °C); WS_II, wind speed 2 m/s; WS_III, wind speed 3 m/s; Side_Inlet, inlet to the installation; Side_outlet, outlet from the installation; RH_S, small relative humidity (RH < 50 %); RH_M, medium relative humidity (51–89 %); RH_B, big relative humidity (90–100 %); NO_3–N, nitrate nitrogen; NO_2–N, nitrite nitrogen; NH_4–N, ammonium nitrogen; PO_4–P, phosphate phosphorus.

* Corresponding author.
E-mail address: piotr.cyganowski@pwr.edu.pl (P. Cyganowski).

[1] PC and ŁG contributed equally to this work.

https://doi.org/10.1016/j.jwpe.2024.104959
Received 9 January 2023; Received in revised form 9 August 2023; Accepted 3 February 2024
Available online 10 February 2024

these water bodies are easily contaminated by the agroindustry [2,3]. Therefore, these policies put considerable pressure on accelerating the reduction of nutrient pollution by scaling effective strategies [4].

Among different factors, such as the production of energy and various goods [5,6], increasing food production and food production rates are recognised as key factors that sustain the growing human population [7]. To achieve increased food production and food production rates, inorganic fertilisers mainly composed of nutrients based on N and P elements have emerged as the basis of modern agricultural strategies [8]. Mineral compounds providing nutrients in the form of NO_3^- and PO_4^{3-} easily decompose in soil, and what is recognised as an advantage in terms of plant nourishment can also result in surface and ground water pollution [9,10]. In this context, fertilisers (often linked with their overuse) constitute the main source of N- and P-based nutrient contamination; N- and P-nutrient contamination is recognised as one of the key factors that reduces the quality of water [8–10]. The problem is critical, because increasing food production affects all parts of the globe, including well-developed or highly populated areas and developing areas. The resultant water contamination poses a severe threat to society [9,11–13].

N contamination caused by NO_3^- can damage O_2 transport in human organisms [14,15]. NO_3^- in drinking water causes methemoglobinemia, diabetes, cancer, reproductive defects, and thyroid disease [11,14,15]. Furthermore, both NO_3^- and PO_4^{3-} are recognised as the main cause of eutrophication of surface waters, leading to biodiversity loss and excessive greenhouse gas emissions [16–21] Thus, there has been extensive research has been devoted to the development of different methods for nutrient removal from water bodies. These include adsorption processes on different materials [22,23], such as clays, carbons, hydroxides, zeolites, chitosan, and most recently, a set of clays [22–24], which have already been used for the removal of NO_3^-. Adsorption processes have also been used extensively for the removal of PO_4^{3-}. To date, various polymers [25], carbons [26], oxides, hydroxides [27], and composites [28] have been used. However, other techniques have been rarely reported, and include *i.a.* electrocoagulation processes for the removal of NO_3^- [29] and PO_4^{3-} [30]. In addition, a set of bio-based methods [31–33] and capacitive deionisation, have been applied for the removal of NO_3^- [34].

One of the technologies that can achieve this goal is ion exchange-based technology. Ion exchange offers selectivity towards the species of nutrients. Moreover, compared with membrane (such as reverse osmosis) and adsorption processes, ion exchange operational costs are much lower and do not require the disposal of a spent adsorbent material [22]. The literature provides examples of bio-aided ion exchange technologies that have been applied to decrease NO_3^- concentration in groundwater [35]. This also includes a pilot-scale setting implemented in the United States in the early 1990s [35,36]. However, the application of ion exchange technology is limited as it increases complications with the treatment of regenerants, which volumes and composition may be a real problem [22]. Moreover, the literature shows that no ion exchange technology has been applied to the treatment of surface waters.

The aim of this study was to improve water quality in pumping station reservoir located in agricultural catchment areas. It was done by developing and implementing a new full-scale ion exchange-based technology for the purification of nutrient contamination. In the context of above-mentioned advantages, we hypothesize, that the development of new technology may be a real solution for the nutrient contamination observed in retention reservoirs all around the world. In respect to other techniques, it could not only be appealing from economic point of view, but also may offer implementing installations in areas with limited access to facilities. For implementing the technology, the *Turawa* reservoir catchment (Opole Province, Poland) was selected as the installation location. This water reservoir perfectly reflects the challenges that prevail globally, because it is localised in the catchment areas of extensive agriculture. The location implies that there is an increased concentration of organic and inorganic compounds of N- and P-nutrient species, which leads to the deterioration of the water quality, and increased eutrophication, and silting.

The implemented technology is characterized by a modular design, in which strong base anion exchange resin (SBA), was packed into a set of 0.2-m^3 columns, which were further put in a container station (2 ion exchange columns in a container). Such an idea makes the installation easily scalable (by adding columns or whole container modules), and allows to set the installation in hard-to-reach areas with limited access to utilities (each container is a self-sufficient unit). Within the research, SBA PA202 resin was used as the core of the technology. This well established commercial product has been already recognised as selective towards NO_3^- species and as such it was hypothesized, that it will be possible to optimize process parameters to make the resin remove other nutrient species as well. Hence, within the implementation we focused on optimizing the bed capacity of the resin for the removal of NO_3^-, and PO_4^{3-}, originating from agricultural catchment areas and water reservoir sediments as well as SO_4^{2-} present in water reservoir. Optimizing the bed capacity was particularly important for implementing the technology for two major reasons. First, the "field" concept excluded any access to facilities like waterworks and sewers; therefore, all the effluents would have to be collected and transported to a sewage treatment plant. Second, treatments of regeneration effluents consisting of brines is a major technological problem, that involves expensive membrane or thermal processes. In this context in this study, time interval between the regeneration of the ion exchange bed was extended, and the reduction of the volume of the column effluents was achieved. This further resulted in the optimal operational and economic process parameters. Finally, the optimised technology was implemented, and the installation environmental impact was assessed over 1-year period. Within this approach, mechanisms of nutrient release and removal were linked and optimised towards tested environmental factors, such as season, air temperature, wind, and relative humidity.

2. Experimental

2.1. Materials and instrumentation

Pure PA202 resin was supplied by Pure Resin Co. Ltd. (Zhejiang, China) in a swollen hydrochloride form and was used as received. Table 1 lists the characteristics of the resin provided by the supplier.

The reagents for the analysis of NO_3^-, PO_4^{3-} and SO_4^{2-} concentrations, *i.e.* sodium salicylate, sodium potassium tartrate, sulfuric acid, molybdic acid, ascorbic acid, standard for the determination of nitrates and phosphates, barium chloride, ammonium chloride, hydrochloric acid, and methyl orange, were purchased from ARCHEM *Sp.* z o.o., Alchem Grupa *Sp.* z o.o. (Torun, Poland). Analytical-grade reagents (or better) and redistilled water were used for the analysis. The on-site research was performed using accessible water (from reservoir).

Attenuated total reflectance Fourier-transform infrared (ATR-FTIR) spectra were acquired using a Jasco FT-IR 4700 instrument (MD, USA) equipped with a diamond ATR module. The spectra were recorded at a resolution of 4 cm^{-1} by applying 64 scans. Scanning electron microscopy (SEM) images were captured using an EVO LS15 Zeiss microscope equipped with an energy-dispersive X-Ray analyser. The spectrophotometric analysis of nutrients was performed using a Thermo Scientific

Table 1
Characteristics of macroporous PA202 resin (Pure PA202 resin datasheet) [63].

Matrix	Styrene-co-divinylbenzene
Functionality	$R–N^+–R_3\ Cl^-$
Sphericity	Min 95 %
Size range	16–50 mesh
Water retention in Cl^- form	52–56 %
Total exchange capacity	1.0 eq. L^{-1}
pH range	0–14

Evolution 220 UV–Visible Spectrophotometer (MA, USA).

2.2. Turawa retention reservoir characteristics

The *Turawa* reservoir is one of Poland's most important basins of this type. It is located at the 18th km of the river *Mała Panew* and its water content is released into the river *Odra*. Fig. 1 shows the location and topography of the basin. The reservoir is 5 km in length and 2.5–4 km in width; it covers an area of 20.8 km^2 and has a 106.2 hm^3 capacity. On its western side, the basin is enclosed by an earthy dam (6 km in length; 13 m in height), which houses a pressure relief system and a hydroelectric power station.

The reservoir *Turawa* has not been cleaned since its launch, and during that time, it collected nutrient contaminants coming down the stream of the *Mała Panew* catchments. The nitrate nitrogen and phosphate phosphorus water pollution of the *Turawa* reservoir is the result of agricultural activities [37–42]. Additionally, in the past, reservoirs experienced a high discharge of household pollutants. This significantly worsened the water quality over the years, and the water quality was negatively affected by the 1997 flood. In the context of nutrient contaminants, the installation was set up in a catchment area after identifying the streams of effluent from the fields (Fig. 1, red dot) located near *Szczedrzyk* village. This location was selected because the watercourse flowing into the *Szczedrzyk* pumping station contains high concentrations of nitrate nitrogen and phosphate phosphorus. These waters are collected in the catchment area's storage tank (Fig. 1) and pumped directly to the *Turawa* reservoir, which results in the water quality deteriorating. Table 2 displays the average nutrient contaminant concentrations determined in the installation in the period–2020–2021.

The values displayed in Table 2 confirm a significant deterioration in water quality. The concentrations of nitrate nitrogen and phosphate phosphorus are calculated as the average seasonal concentration values, where season 1 (S1) is spring, season 2 (S2) is summer, season 3 (S3) is autumn and season 4 (S4) is winter. The colours indicate water quality classes in accordance with Polish law. Blue indicates class I water quality, and green indicates class II water quality. In the two year study period, nitrate nitrogen concentrations in S1–S4 of 2020 and S1 of 2021 were above class I of water quality defined in accordance with Polish regulations (Table 2) [62]. The range of nitrate nitrogen concentrations in the study period 2020–2021 ranged from 0.75 to 4.03 mg L^{-1} (Table 2). Phosphate phosphorus concentrations exceeded class I water quality in S2 in 2020 and in S1–S2 in 2021 [62]. The range of phosphate phosphorus concentrations in the study period 2020–2021 ranged from 0.02 to 0.12 mg L^{-1} (Table 2). In this context, the *Turawa* reservoir can serve as an example of surface waters occurring globally; hence, implementing a successful technology for its purification could broaden the perspectives of Earth's water preservation and sustainability.

Table 2
Seasonal average nutrient contaminant concentrations (mg L^{-1}) in installation setting located in *Szczedrzyk* catchment area in 2020–2021.

Season (S1-S4)*	NO_3-N	PO_4-P
S1 of 2020	2.47	0.06
S2 of 2020	2.98	0.10
S3 of 2020	2.34	0.02
S4 of 2020	3.42	0.02
S1 of 2021	4.03	0.12
S2 of 2021	1.12	0.08
S3 of 2021	0.75	0.03
S4 of 2021	1.80	0.06

*S1-spring; S2-summer; S3-autumn; S4-winter
Water quality (according to Polish regulations): **blue-class I**; **green-class II**

2.3. Ion exchange technology and installation

The installation was set up in the form of container stations equipped with ion exchange columns and the necessary equipment, which will be described further in this section. Fig. 2 displays photographs of the installation set up in the *Szczedrzyk* catchment area. Fig. 3 shows the design of the installation operation.

In general, the installation design involved a *twin* configuration of the water purification station. This implies that the container station contained one pair of ion exchange columns. While one of them was involved in water purification, the second was regenerated and *vice versa.* Additionally, a mechanical filter (3rd column filled with sand, denoted as F1 in Fig. 3) was applied as a pre-filter before introducing water onto the ion exchange columns.

The operation of the setting begins with the collection of raw water through a suction filter (perforated tube with a diameter of 10 cm and length of 50 cm, F1, Fig. 3). The water was then transported through a pipe (4 cm in diameter) using a suction pump controlled by an inverter (PO, Fig. 3) and introduced into a mechanical filtration column (quartz sand gravel bed, F1, Fig. 3). Thereafter, the pre-filtered water was introduced onto an anion exchange resin bed packed into 200 L columns set in *twin* mode, as described above. Each of the ion exchange columns (F2/F3, Fig. 3) was equipped with a control head, RX116A3 (RX, Poland), responsible for the automatic control of the filtration and regeneration processes. After purification, the processed water was transferred to the reservoir. Each ion exchange column was equipped with separate containers for the regenerant (ZZR, Fig. 3).

Resin regeneration was performed after the resin capacity (determined by breakthrough curves) was exhausted. This was performed in the following manner. First, the resin bed was backwashed using water from reservoir, at a flow rate of 49.2 L min^{-1}. Second, in the container denoted as ZZR (Fig. 3) a 75 dm^3 of saturated NaCl brine was prepared.

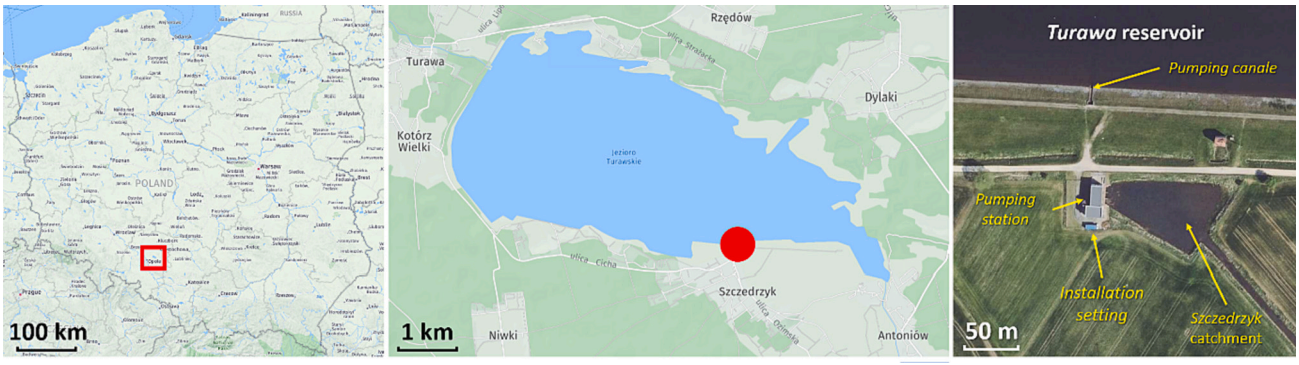

Fig. 1. Location and topography of *Turawa* reservoir. Red dot denotes location of ion exchange installation. Maps acquired from HERE WeGo and Geoportal.gov.pl. (For interpretation of the references to colour in this figure legend, the reader is referred to the web version of this article.)

Fig. 2. Photographs of container station set in the *Szczedrzyk* catchment area.

The prepared solution was collected in a Venturi tube into a column head (Fig. 3), where the brine was diluted approximately twice and passed through the column at a rate of 1.89 L min^{-1}. This resulted in the passage of 1 BVs of the regenerating solution through the column, which was collected in a 1 m^3 pallet mauser-type container (Fig. 2, ZP in Fig. 3), and utilised in sewage treatment plant. Third, the resin bed was backwashed again. The prepared resin was used in the next cycle of purification.

Other considerations:

a. Joints between columns were equipped with check and shut-off valves
b. Both the mechanical filtration and ion exchange columns were equipped with a three-way valve to control the filtration and regeneration steps of the process.
c. Both the filtration and regeneration processes were performed in a counterflow. A backwash was applied between the processes.
d. The regeneration of the mechanical filter involved a sand-bed backwash using raw water. The effluent was returned to the retention reservoir.
e. The outflow from the ion exchange column was measured with a water metre to determine the actual installation performance.
f. Water circulation in the entire installation was driven by a pump with a nominal capacity of 10 m^3. One pair of ion exchange columns worked with a capacity of 5 m^3 h^{-1} and the full capacity of the pumps was used only during regeneration.
g. The installation works under a pressure of 3.5 bar (the pressure sensor and pressure equalisation tank are located directly behind the pump).
h. All columns had a volume of 200 L and were filled to approximately 70 % of their capacity.
i. The bottom of the ion exchange columns contained approximately 20 L of gravel and 140 L of ion exchange resin.
j. All elements of the installation were connected with plastic pipes with a diameter of 40 mm.
k. The installation works in continuous mode (24 h a day, 7 d a week)

Within the described design, the water purification technology could be easily expanded by setting up additional container stations that could readily increase the water purification efficiency and be installed at various locations around the retention reservoirs.

2.4. Optimisation of nutrient sorption and water purification

The purification process was optimised at the location *Szczedrzyk* (Fig. 1) under the actual operating conditions of the installation. Optimisation was performed with NO_3^- and PO_4^{3-} ions as representative N- and P-bearing nutrients. Additionally, although SO_4^{2-} ions occur naturally in water, their concentrations are also considered in terms of water purification process parameters. Optimisation was performed by drawing breakthrough curves of an anion exchange column (Fig. 2), expressed as (1):

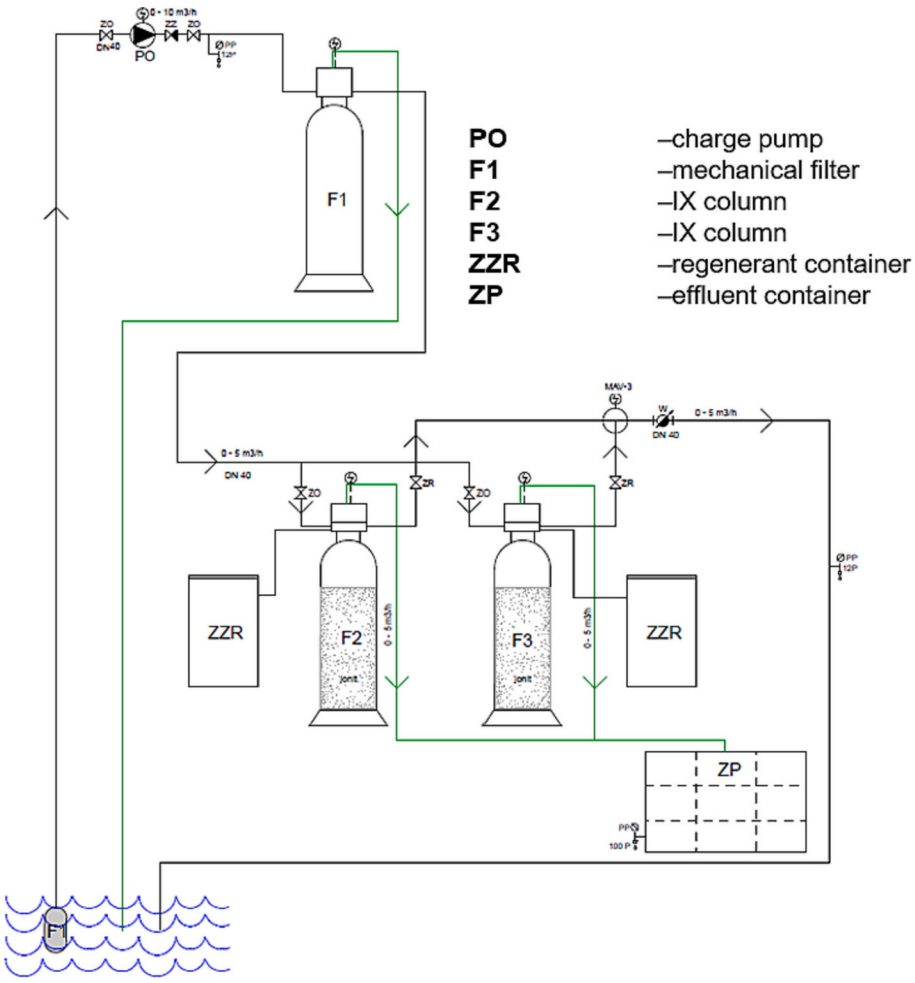

Fig. 3. Water purification installation scheme.

$$\frac{C_e}{C_0} = f(BVs), \tag{1}$$

where C_e and C_0 are the concentrations (mg L^{-1}) of NO_3^-, PO_4^{3-} and SO_4^{2-} at the outflow of the column and in the feed water before purification, respectively. In turn, *BVs* is the volume of purified water expressed as the number of resin bed volumes (0.14 m^3). Because the optimisation was performed under the actual conditions of the installation operation, the concentrations of the nutrients in the feed water changed over time. Thus, data were collected in the following manner. Samples of raw water were collected every 1 h of the process duration before entering the column, while the samples of the column outflow were collected every 15 min of the process duration. This corresponds to 5 and 1.25 m^3 of passed water, respectively. The ratio of C_e/C_0 was calculated using C_e and C_0 values collected in the same sets of samplings. This allowed us to consider the estimated C_0 value that passed through the column. The process was performed until equilibrium of C_e/C_0 was achieved. The collected data points were then fitted using a sigmoidal function. The working capacities of the resin were calculated by integrating the area above the breakthrough curves [43] using Origin Pro 2021 software.

2.5. Methodology of environmental research

The research site was located in the *Turawa* catchment reservoir at the pumping station in *Szczedrzyk*. For the installation located in the reservoir area, two sampling sites were established: (1) inlet of water at the *Szczedrzyk* pumping station that is transferred to the installation (inlet), and (2) outlet of the treated water that is transferred from the installation to the *Szczedrzyk* pumping station reservoir (outlet). During the entire research period, the anion exchange column at the installation was not replaced. It was assumed that it would be optimal to conduct research and evaluate the selected physicochemical parameters over a period of two years. The sample points for the concentrations of nitrate nitrogen (NO_3–N), nitrite nitrogen (NO_2–N), ammonium nitrogen (NH_4–N), total Kjeldahl nitrogen (TKN), organic nitrogen (ON), total nitrogen (TN), phosphate phosphorus (PO_4–P), total phosphorus (TP), dissolved oxygen (DO), five-day biochemical oxygen demand (BOD_5), chemical oxygen demand (COD_{Mn}), total suspended solids (TSS), and dissolved substances (TDS) were collected from the edge of the storage tank of the pumping station using scoops (water from the littoral zone and water within the tested installation). The electrical conductivity of water (EC) and the pH were measured *in situ*. Water samples were not taken while the pumping station was running, during periods of technological breaks and power outages, and when the reservoir was frozen. Samples from the period 2020–2021 are presented in the environmental studies. Water samples were collected considering the randomness and seasonality of the tests, especially the cyanobacteria blooms occurring during reservoir freezing. A total of 202 water samples were taken in August and November to reveal the efficacy of the installation operation when the cyanobacteria bloom was the largest and after the vegetation period. Consequently, water samples were mainly taken in the months of March and May (2021), June and August, and September and November to reveal the effectiveness of the installation in spring, summer, and autumn, respectively.

Table 3 presents the methodologies used to test the selected physicochemical indicators, standards, limits of quantification, and detection

Table 3
List of standards and research methodology.

Pollution indicator[a]	Methodology	Standard	Limits of quantification	Detection limits
NO_3–N	Spectrophotometric method	PN-82C-04576/08	0,05 mg L^{-1}	0,007 mg L^{-1}
NO_2–N	Spectrophotometric method	PN-EN 26777:1999	0,001 mg L^{-1}	0,0003 mg L^{-1}
NH_4–N	Spectrophotometric method	PN-ISO 7150:2002	0,01 mg L^{-1}	0,003 mg L^{-1}
TKN	Specific method	PN-EN 25663:2001	0,01 mg L^{-1}	0,003 mg L^{-1}
PO_4–P	Spectrophotometric method with ammonium molybdate	PN-ISO 6878:2006	0,01 mg L^{-1}	0,005 mg L^{-1}
TP	Spectrophotometric method with ammonium molybdate (mineralisation with HNO_3 i H_2SO_4)	PN-EN 1189-2000 PN-EN ISO 6878:2006	0,01 mg L^{-1}	0,005 mg L^{-1}
DO	Iodometric method	ISO 5813:1983	0,5 mg L^{-1}	0,1 mg L^{-1}
BOD_5	Specific method	PN-EN 1899-1:2002	0,5 mg L^{-1}	0,1 mg L^{-1}
COD_{Mn}	Specific method	PN-EN ISO 8467:2001	0,5 mg L^{-1}	0,2 mg L^{-1}
TSS	Weight method	PN-EN 872:2007	5 mg L^{-1}	< 5 mg L^{-1}
TDS	Calculation method	PN-C-04616/01	5 mg L^{-1}	< 5 mg L^{-1}
pH	Potentiometric method	PN-90/C-04540.01	1,0–12,0	0–14
EC	Conductometric method	PN-EN 27888:1999	2 µS cm^{-1}	< 2 µS cm^{-1}

[a] NO_3–N: nitrate nitrogen; NO_2–N: nitrite nitrogen; NH_4–N: ammonium nitrogen; TKN: total Kjeldahl nitrogen; ON: organic nitrogen; TN: total nitrogen; PO_4–P: phosphate phosphorus; TP: total phosphorus; DO: dissolved oxygen; BOD_5: five-day biochemical oxygen demand; COD_{Mn}: chemical oxygen demand (permanganate index); TSS: total suspended solids; TDS: dissolved substances; EC: electrical conductivity

of the tested indicators.

The influence of seasonal changes and meteorological parameters on the physicochemical parameters determined at the inlet and outlet, including the concentrations of NO_3–N and PO_4–P, was investigated using redundancy analysis (RDA). The descriptors were transformed to meet the assumptions of RDA normality, except precipitation (P), wind speed (WS), wind direction (WD), air temperature (AT), and relative humidity (RH). The predictor variables were significant at $p \leq 0.05$, as determined by the Monte Carlo permutation method (1000 permutations).

3. Results and discussion

3.1. Anion exchange resin characteristics

The SBA resin used in the installation exhibited the characteristics provided by the supplier which are displayed in Table 1. The morphology was assessed and confirmed using SEM/EDX; the corresponding photomicrographs and elemental compositions are shown in Fig. 4. The EDX spectrum is shown in Supplementary Fig. S1.

As shown in Fig. 4, the morphology of the PA202 resin is uniformly spherical with no crushed pearls (Fig. 4A). The diameters of the polymer beads range from 0.4 to 1 mm (Fig. 4A-C). The surface is mainly smooth (Fig. 4B,C), with some visible inclusions. This can be linked to the presence of Na and Ca detected by EDX analysis (Fig. 4D, Fig. S1). The Na and Ca can originate from NaCl or $CaCl_2$ as these compounds are usually used for saturates the water phase applied during suspension polymerisation [44]. In addition, the EDX analysis confirms the presence of C, which is the major component in the material (Fig. 4D). This element originates from the polymer itself. The analysis also indicates the presence of O, which could originate from the hydrolysed -CH_2Cl groups present in the polymeric matrix or from –OH groups that could be present in the matrix itself or in the structure of the resin functionalities [44]. Because the EDX is not sufficient to confirm the presence of N [64], which could indicate the amino functionalities declared by the supplier, the chemical structure of the PA202 resin was additionally confirmed by performing ATR-FTIR measurements and analysis of the obtained

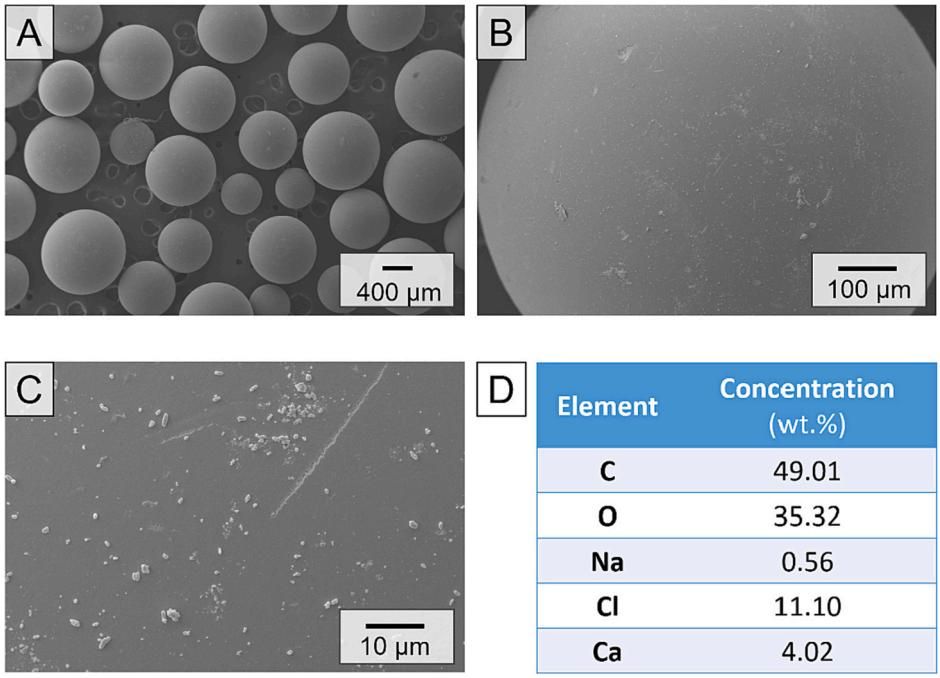

Fig. 4. SEM analysis of unused Pure PA202 resin. (A-C) SEM photomicrographs, (D) elemental composition obtained from the EDX spectrum. EDX spectrum is provided in supplementary materials as Fig. S1.

spectra. The results are shown in Fig. 5.

Based on the spectra, multiple functional groups and structural elements of the measured samples could be identified. The band at 677 cm^{-1} can be attributed to the chloromethylene group (–CH_2Cl) [45]. Slightly higher, at 786 cm^{-1} we observe an aliphatic backbone scissoring (–CH_2) band. Three bands (1394, 1454, 1633 cm^{-1}, respectively) suggest the presence of conjugated = C–C = bonding in the analysed resin. A similar band alignment in this region was observed for S-co-DVB in a previously reported study [46]. Two peaks are recognised in the upper wavelength region (2984 and 2920 cm^{-1}); the former can be assigned to pendant ethylbenzene group stretching, while the latter indicates an aliphatic C—H stretching mode [47]. The high-intensity band located at 3356 cm^{-1} can be assigned to –OH stretching (derived from hydrolysed –CH_2Cl groups) as well as N—H deformation vibrations in the primary and secondary amines [48]. Although FT-IR is not sufficient for determining the structure of the functionalities present in the PA202 resin, the recorded spectrum shows a series of N—H and C—N vibrations at 1610, 1176, and 1145 cm^{-1}, respectively (Fig. 5). These results suggest that the anion exchange resin is loaded with amino moieties; thus, the water purification process may depend on anion exchange on the amino functionalities. For guidance, the anticipated reactions are provided in the supplementary information in Figs. S2-S4.

3.2. Process optimisation

The process parameters were optimised by plotting the breakdown curves of the ion exchange column under actual operating conditions at the *Szczedzrzyk* location. The breakthrough curves presented in Fig. 6 express the ratio of the equilibrium and initial concentrations (C_e/C_0) of the removed nutrients as a function of the number of bed volumes (BVs). During the sampling period, the mean concentrations of the analytes in the treated water were 13.2 ± 2.88 mg NO_3^- L^{-1}, 86.2 ± 20.36 mg SO_4^{2-} L^{-1}, and 0.12 ± 0.015 mg PO_4^{3-} L^{-1}.

The determined breakthrough curves of the column (Fig. 6) show that the PA202 resin is selective for NO_3^- ions. The removal efficiency thereof was 93–100 % ($C_e/C_0 \approx 0$) during water filtration to 560 BVs (approximately 100 m^3 of filtered water). Subsequently, a column breakthrough occurred. This was observed by the gradual increase in the shape of the NO_3^- equilibrium concentration in the C_e/C_0 expression (Fig. 6). In this area (BVs > 560), nitrate removal efficiencies of 60, 50, 20 %, and 7 % are observed for BVs of 730, 843, 916, and 1010, respectively, corresponding to 130, 150, 163, and 180 m^3 of filtered water, respectively. The complete breakthrough of the column, in which the equilibrium concentration of NO_3^- is brought into line with its initial concentration, that is, $C_e/C_0 = 1$ is observed at BVs = 1085, which corresponds to 193 m^3 of filtered water. The area above the breakthrough curves allows for the estimation of the maximum loading capacity of the resin bed [43]. Based on this it is estimated that the column

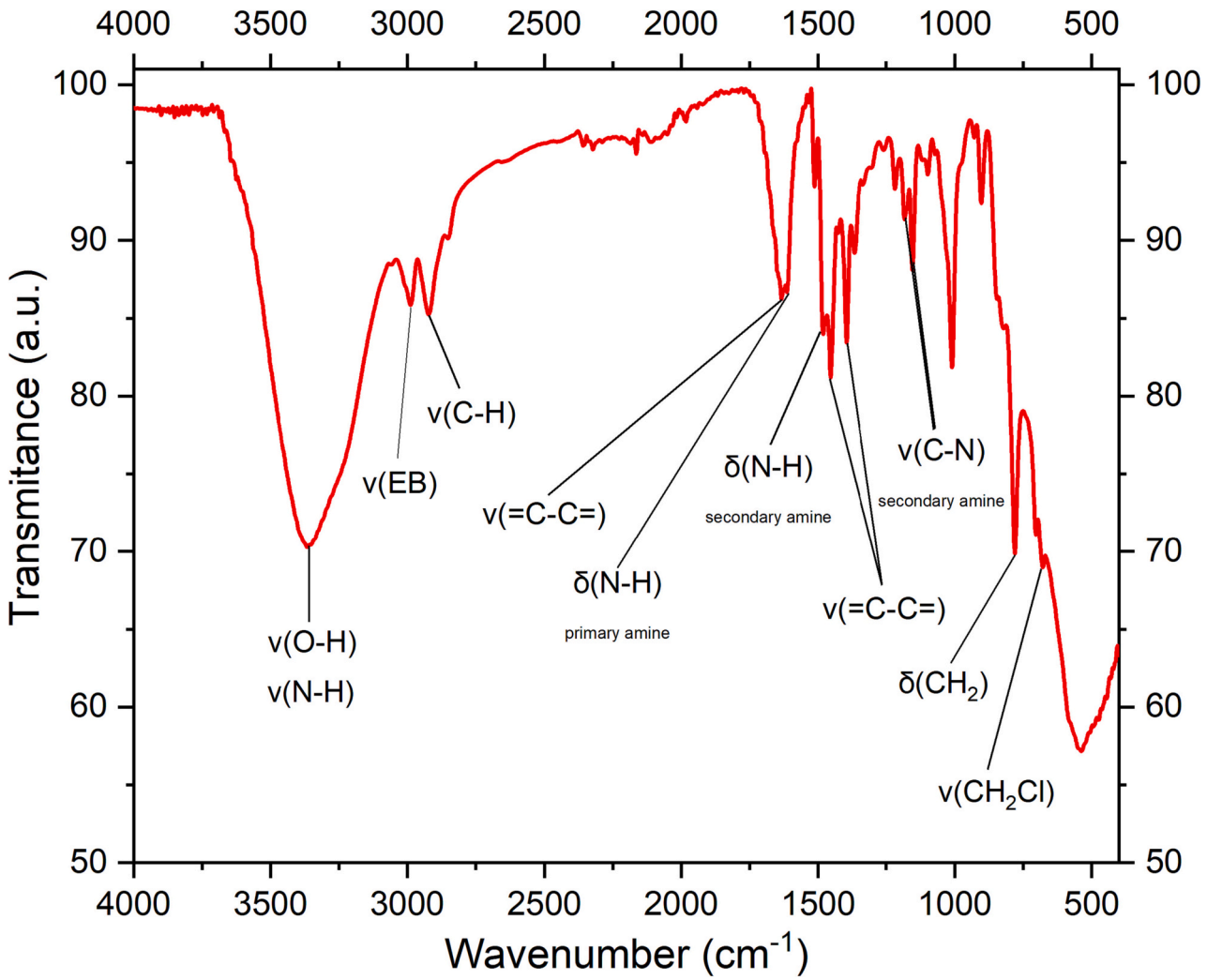

Fig. 5. ATR-FT-IR spectrum of PA202 resin. Abbreviations: stretching bands (ν), scissoring band (δ), ethylbenzene group (EB).

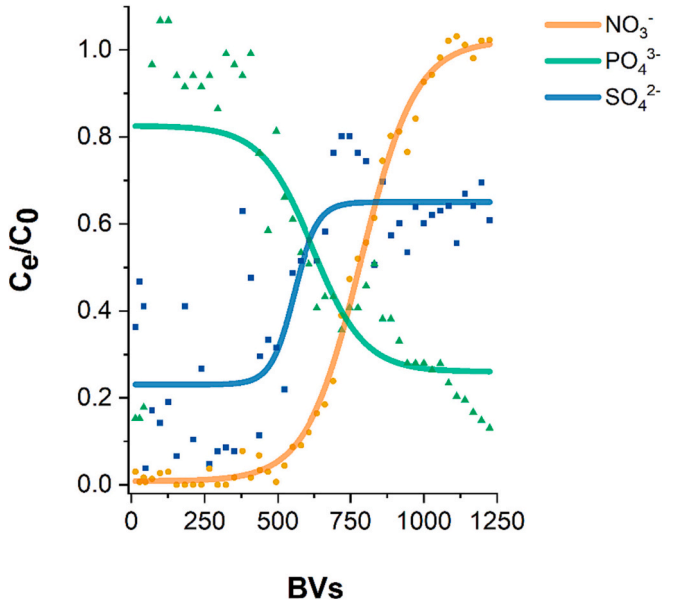

Fig. 6. Breakthrough curves of optimised anion exchange column. Data were collected in real conditions of installation operation. C_e: concentration of nutrients in outflow, C_0: initial nutrient concentration, BVs: number of resin bed volumes. Average initial concentrations: 13.2 ± 2.88 mg NO_3^- L^{-1}, 86.2 ± 20.36 mg SO_4^{2-} L^{-1}, and 0.12 ± 0.015 mg PO_4^{3-} L^{-1}. Data points were approximated using sigmoidal function using OriginPro 2021 software.

removed 1779 g of NO_3^- which is equal to 401.7 g of N, and 0.16 eq–NO_3^- L^{-1} (the importance of these values will be discussed further in the manuscript).

The efficiency of SO_4^{2-} ion removal in the initial stage of the water purification process was determined to be 38–97 %. After the NO_3^- ions broke through the column (Fig. 6), the SO_4^{2-} removal efficiency was 25–45 %. Fig. 6 shows the significant differences in the profiles of the column breakthrough curves with NO_3^- and SO_4^{2-} ions. Comparing these separate processes, it can be concluded that the removal of SO_4^{2-} from water was less efficient than that of NO_3^-. Moreover, the results for SO_4^{2-} removal varied widely (Fig. 6), while the NO_3^- breakthrough curve was more uniform. This suggests that the SO_4^{2-} needed more time to access the resin's surface, and thus, it must have been susceptible to flow rate and concentration changes that occurred in the real conditions of the installation operation. As a result, the NO_3^- anion was more competitive in accessing the functional groups. A similar observation was made for the removal of the PO_4^{3-} anions. In this case, however, complete breakthrough of the column was observed just after 8 m^3 (~57 BVs) of water passed (Fig. 6). After this initial puncture, the efficiency of PO_4^{3-} removal began to increase as NO_3^- and SO_4^{2-} adsorption decreased (Fig. 6). As a result, 87 % PO_4^{3-} removal efficiency was achieved in the final steps of the process, ensuring the breakthrough curve appears in a reversed shape (Fig. 6).

This phenomenon, *i.e.* gradual decrease in the C_e/C_0 ratio for PO_4^{3-} anions, was inversely proportional to the observed breakthrough of the column by NO_3^- and SO_4^{2-} ions (BVs > 560, Fig. 6). This occurrence suggests that although the capacity of the resin towards NO_3^- and SO_4^{2-} was exploited, it still had functionalities available for PO_4^{3-}. This observation was the basis of the installation modification, which is described in the next paragraph. Based on the results it was concluded that the column with PA202 resin removed approximately 10 kg of SO_4^{2-} anions that was equal to 0.58 eq SO_4^{2-} L^{-1}. In turn, the column removed 11 g of PO_4^{3-} which was equal to 3.6 g of P, and 1.8 × 10^{-3} eq PO_4^{3-} L^{-1}. The summarised gram-equivalents (*eq*) calculated for all the species was 0.73 eq. L^{-1} (0.16 + 0.58 + 0.0018); hence, there is indeed capacity left, as the maximum loading of the resin declared by the supplier is 1 eq. L^{-1} (Table 2). However, based on the profiles of the breakthrough curves (Fig. 6), the remaining capacity was available for PO_4^{3-}.

This observation is important because there are no resins on the market dedicated to the separation of PO_4^{3-}. As indicated by the results, the resin PA202 could remove this anion after it reached equilibrium for NO_3^- and SO_4^{2-} adsorption. This suggests that the resin may be effective in the purification of PO_4^{3-} from water however, we hypothesized that, to achieve this, the water should be pre-purified by removing NO_3^- and SO_4^{2-}. In this context, it would be beneficial to apply a cascade setting for installation. For this reason, we changed the configuration of the setting displayed in Fig. 3, *i.e.* we connected the ion exchange columns, denoted as F2 and F3, into a cascade instead of *a twin* connection. These results confirmed this hypothesis. Column F2 (Fig. 3) removed up to 100 % of NO_3^- and 80 % of SO_4^{2-}, leaving PO_4^{3-} unremoved. Subsequently, pre-purified water was introduced into the second-in-row column F3 (Fig. 3), where 100 % PO_4^{3-} removal was achieved.

In summary, based on the obtained results, it can be concluded that the PA202 resin prefers the loading of NO_3^- over other species. There are interrelationships between the removal efficiencies of individual analytes. They enable further modelling of the process and alteration of the installation configuration, leading to maximum exploitation of the capacity of the resin. However, from an economic perspective, which includes operational costs of processes, such as effluent utilisation, cleaning the filters, supervision, and other service-related maintenance activities, exploiting the resin's capacity to the maximum was pointless. Based on the breakthrough curves, considering the relationships between the removal of analytes, installation efficiency, and the above-mentioned economic factors, the installation was finally set with two columns linked in parallel (Fig. 2), with the volume of purified water set at 160 m^3 between regeneration cycles. This allowed for the satisfactory removal of nutrients and guaranteed an adequate column operation time before regeneration was required.

3.3. *Water purification effect*

Water content was analysed before the inflow and after the outflow from the installation to improve its quality. The installation reduced the concentrations of NO_3-N and PO_4-P in the water of the *Szczedrzyk* pumping station's storage tank. The installation resulted in a reduction in NO_3-N and PO_4-P concentrations in the water of the storage tank of the pumping station. Therefore, the proportional effects of reducing concentrations of NO_3-N and PO_4-P were determined.

In the first series of tests, the concentration of NO_3-N decreases by 97

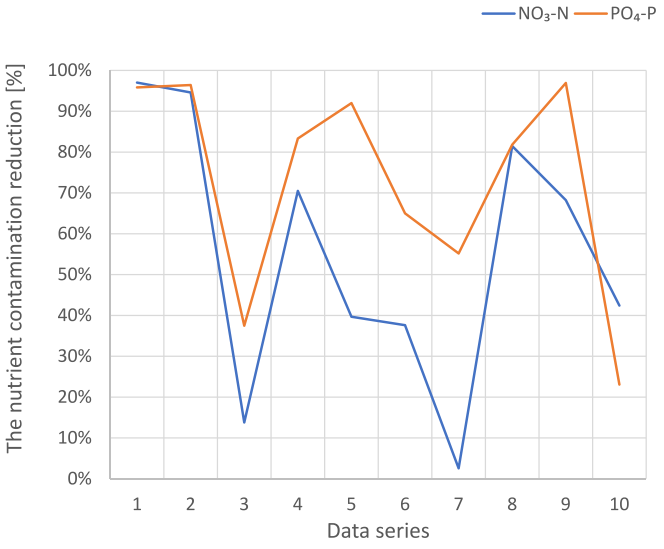

Fig. 7. Percentage effects of reducing concentration of NO_3-N and PO_4-P in water of storage tank of pumping station at *Szczedrzyk* installation (period 2020–2021).

% and the concentration of PO_4-P decreases by 96 % (Fig. 7). The proportional effect of reducing the concentration is more pronounced for NO_3-N than for PO_4-P. In the second series, an inverse relationship is observed. The proportional effect of reducing the concentration is more evident for PO_4-P (96 %) than for NO_3-N (95 %). From the second to the fourth series, fluctuations in NO_3-N and PO_4-P concentrations are noted. However, the recorded PO_4-P proportional effect of reducing the concentration is greater than that of NO_3-N (Fig. 7). In the fourth series, the proportional effect of NO_3-N is 70.5 % and that of PO_4-P is 83 %, respectively (Fig. 7). In the fifth series, it is noted that the concentration of NO_3-N decreases (the reduction efficiency of this compound decreases by 40 %) and the concentration of PO_4-P increases (the reduction efficiency increases to 92 %). In the sixth and seventh series, a decrease in the proportional effect of reducing the concentrations of NO_3-N (up to 3 % in the seventh series) and PO_4-P (up to 55 % in the seventh series) is observed. In the eighth series, an increase in the proportional effect of reducing the concentrations of NO_3-N (81 %) and PO_4-P (81.5 %) is recorded (Fig. 7). In the ninth series, the opposite phenomenon is observed in comparison with the fifth series: the concentration of NO_3-N increases (the proportional effect of the reducing concentration decreases to 68 %) and the concentration of PO_4-P decreases (the proportional effect of the reducing concentration increases by 92 %). In the tenth series, the removal efficiencies of both the compounds decrease. However, an increase in the proportional effect of reducing the

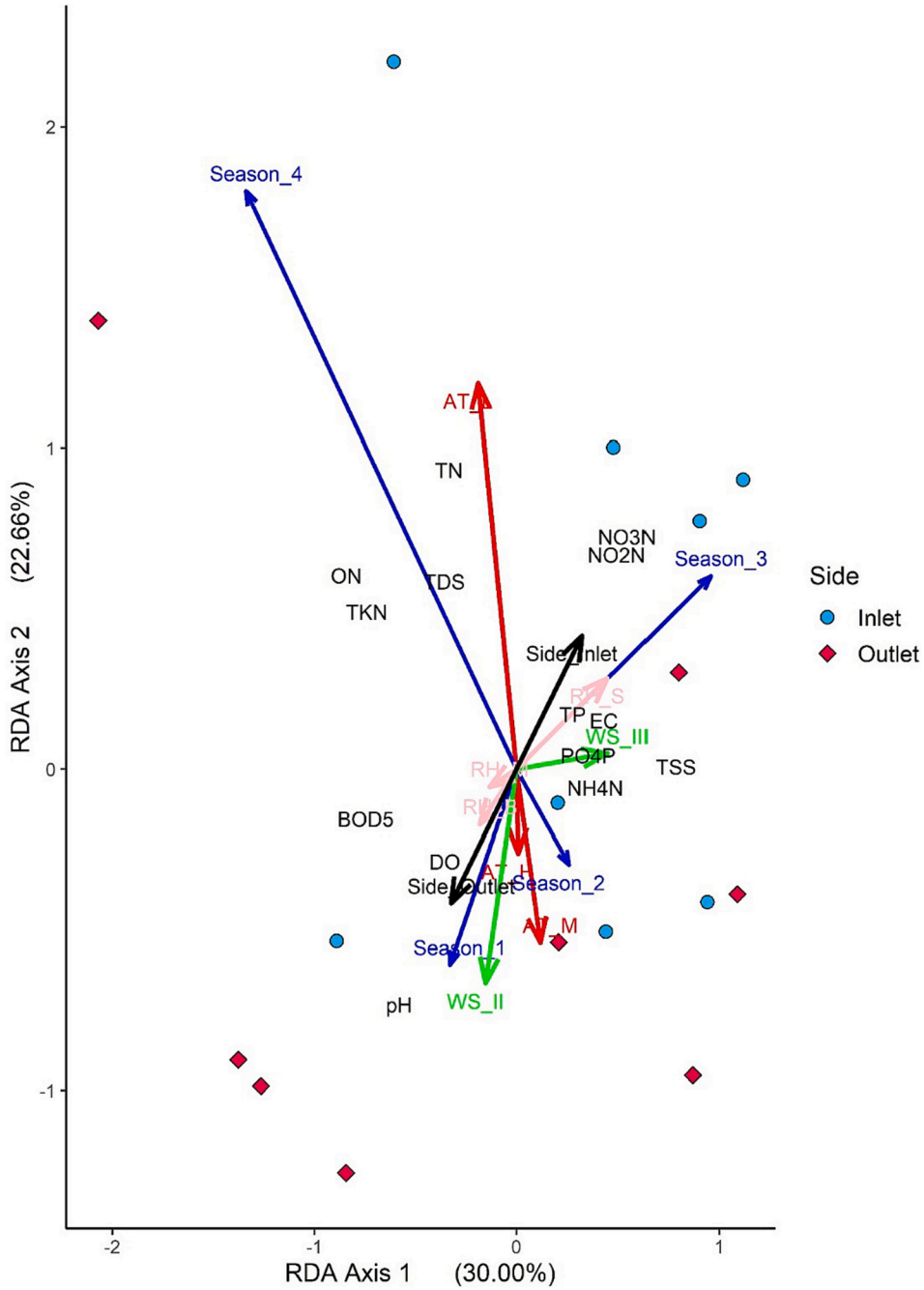

Fig. 8. RDA triplot presenting effects of environmental factors on water quality indices in storage tank of *Szczedrzyk* pumping station. Legend: Season_1 – spring; Season_2 – summer; Season_3 – autumn; Season_4 – winter; AT_L – low air temperature (0–10 °C), AT_M – medium air temperature (11–20 °C); AT_H – High air temperature (21–30 °C); WS_II –wind speed 2 m/s; WS_III – wind speed 3 m/s; Side_Inlet - inlet; Side_outlet – outlet; RH_S - small relative humidity (RH < 50 %); RH_M - medium relative humidity (51–89 %); RH_B - high relative humidity (90–100 %).

concentration of NO_3-N (42 %) and a decrease in PO_4-P (23 %) are observed (Fig. 7).

It should be noted that the concentrations of NO_3-N and PO_4-P were determined in the waters of the storage tank of the pumping station and not in the waters directly discharged from the installation (tap intake). Thus, the water from the storage tank of the pumping station could be mixed with the water from the installation.

The analysis in Fig. 7 shows that the water collected from the expansion tank of the pumping station is also influenced by other environmental factors. Seasonal changes and meteorological parameters were selected among the environmental factors. Redundancy analysis was used to explain the influence of seasonal changes and meteorological parameters on changes in the removal efficiencies of NO_3-N and PO_4-P. This allowed us to identify the meteorological factors that played an important role. The indicators in the RDA analysis were seasonality (season), precipitation (P), air temperature (AT), wind speed and direction (WS, WD), and relative humidity (RH) (Fig. 8).

Five environmental factors: measurement site ($p = 0.030$), wind speed ($p = 0.024$), season ($p = 0.002$), air temperature ($p = 0.033$), and relative humidity ($p = 0.001$) significantly influenced the water quality parameters.

The first two axes (RDA 1 and RDA 2) explained 52.66 % of the variance (30 % and 22.66 %, respectively). Among the environmental parameters, the season type had the greatest impact on the tested water quality indicator. Spring, summer, and winter (S1, S2, and S4) were strongly correlated with RDA 2, while autumn (S3) was correlated with RDA 1. In S4, the following indicators increased: ON, TKN, TDS, and TN, whereas in S3 and S4, the levels of NO_3-N and NO_2-N increased. Seasonality did not affect the presence of NH_4-N. Therefore, it can be assumed that in autumn and winter, there is an increase in the concentrations of organic nitrogen forms associated with the end of the vegetation period of the macrophytes growing on the banks of the reservoir. This is in line with the results obtained by Wall et al. [49] who reported that high denitrification occurs in shallow reservoirs, and is due to the high content of organic matter and nitrogen in the sediments and the high content of NO_3-N in the reservoir water. In turn, the research by David et al. [50] indicated that approximately 58 % of the nitrate nitrogen (NO_3-N) supply to Lake Shelbyville reservoir (Illinois, USA) was removed in spring and early summer. Denitrification, occurs at a low concentration of dissolved oxygen [51], in spring and summer, which was confirmed by these studies (Fig. 8). Thus, this would explain the NO_3-N increase in autumn and winter.

Seasonality is related to air temperature, the decrease of which was demonstrated in the autumn-winter seasons ($0\ ^\circ C \leq AT\_L \leq 10\ ^\circ C$) and the increase which was noted in the summer-spring seasons ($11\ ^\circ C \leq AT\_M \leq 20\ ^\circ C$, $21\ ^\circ C \leq AT\_H \leq 30\ ^\circ C$). The influence of temperature on water quality indicators is similar to that of seasonality, with the lower temperatures having a greater significance. The air temperature has a significant influence on the solubility of oxygen in water. The dissolved oxygen content decreased with increasing temperature. The resulting decrease in oxygen levels may increase the denitrification rate [51]. The *in situ* degradation of biomass (green algae and diatom biomass deposition and death of macrophytes in autumn) may also contribute to the release of nitrogen forms. The decomposition of organic matter followed by denitrification increases the nitrogen content [52] in autumn and winter.

The wind had a significant influence on pH, DO, EC, TSS, and forms of phosphorus (PO_4-P and TP). The increase in wind speed significantly influenced the increase in water aeration and reduction in pH from 10 to 8. Thus, increased wind speed ($WS\_III = 3$ m/s) causes movement and oxygenation of the water and improves its quality, which is consistent with the research by Pompeii et al. [53]. The deterioration of water quality was demonstrated for the phosphorus forms, PO_4-P, TP, EC, and TSS, the levels of which increased with increasing wind speed. In their study, Pompeii et al. al. [53] and Chalar and Tundisi [54] showed that an increase in wind speed affects the maximum re-suspension of solid particles and organic matter; hence, it has an impact on the growth of suspension in the water of the reservoir. Moreover, as reported by Huang et al. [55], wind-driven sediment re-suspension exerts a significant influence on the behaviour of the phosphorus compounds. The increase in wind speed increases the re-suspension of sediments and the release of phosphorus from the bottom sediments of shallow-water reservoirs. Research by Jindal and Wats [56] showed a correlation between changes in EC concentration and wind. However, these studies were performed in India. The influence of air and wind temperatures on the concentration of total phosphorus in the water of the shallow Yuqiao Reservoir (China) was significant in summer and autumn [57]. The tested factor, relative humidity, manifested in the opposite way to the action of wind–higher wind–lower humidity. Thus, reduced humidity favours higher indices of phosphorus forms and higher EC and TSS levels.

Regarding the operation of the installation, it has been shown that the level of operation of the installation is influenced by other environmental factors such as the season, temperature, wind, and air humidity. The installation worked most optimally (considering the impact on nitrogen forms) in season 1 (spring, with an average air temperature of $11\ ^\circ C \leq AT\_M \leq 20\ ^\circ C$, high relative humidity–$RH\_B = 90$–100 % and medium wind ($WS\_II = 2$ m/s)).

3.4. Challenges and future improvements

The design process and installation have led to the development of a new technology for the purification of nutrient contaminants from water. Although the results presented here focus on the development, optimisation, and purification efficiency of one container station (*Szczedrzyk*, see Fig. 1), the technology is currently implemented with success at other stations placed around the *Turawa* reservoir (see Fig. 1). Within the implementation, it was possible to define the optimal operating conditions to maximise the interval between the regeneration of the ion exchange resin bed, and to determine the nutrient loading capacities. This context is particularly important, as it may allow for the development of a new strategy for the re-utilisation of column regeneration effluents.

The water treatment and resin bed regeneration strategies were monitored by assessing the water purification efficiency at constant time intervals. For almost a year, the applied conditions and operating parameters resulted in good purification factors. However, after approximately one year of installation, we observed a significant decrease in the efficiency of the water purification. This observation was linked to the summer season, when intensified eutrophication of the water reservoir occurred. To determine the cause of this phenomenon, resin samples were collected directly from a column and subjected to SEM/EDX analysis. The results are shown in Fig. 9. The EDX spectrum is provided in the supplementary material (Fig. S2).

After opening the column, a characteristic scent associated with the decomposition of organic matter was detected. As can be seen in Fig. 9, the morphology of PA202 after 1 year of operation is significantly different from that of the unused sample (Fig. 4). Based on the photomicrographs, it can be concluded that the observed substance covering the polymer grains probably blocks access to the active surface of the material. At this point, it should also be mentioned that after 1 year of operation, we did not observe excessive breaks and cracks in the resin grains, which suggests the high mechanical strength of the resin. Along with the assessment of the surface topography, the elemental composition was also analysed. As shown in Fig. 9E and compared with Fig. 4D, an increased share of O was observed and the presence of a number of metals, which were not detected in the unused sample (Fig. 4D) was noted. The differences in the elemental compositions suggest that the material observed on the surface of the resin may be a mixture of organic and inorganic impurities, the elemental composition of which conforms with the impurities present in the *Turawa* reservoir. It should also be noted that the resin obtained from the ion exchange column has a much

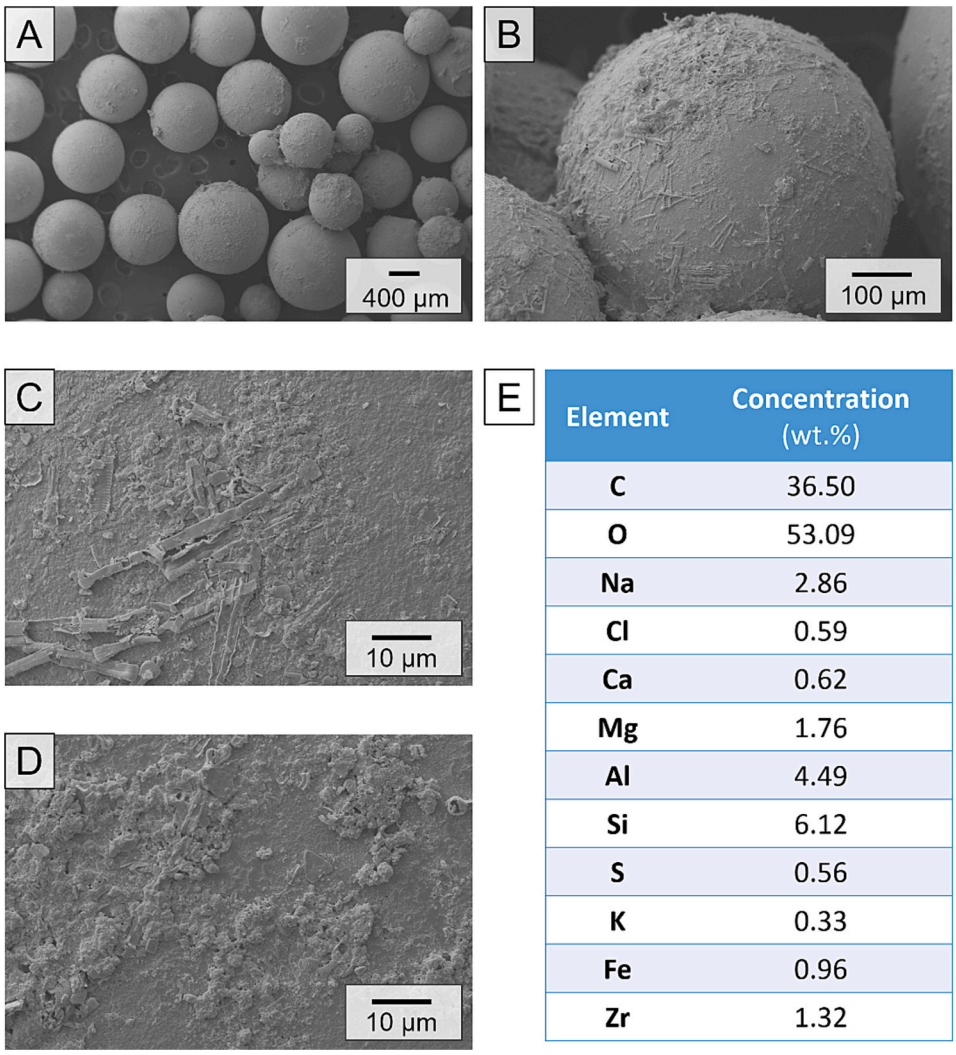

Element	Concentration (wt.%)
C	36.50
O	53.09
Na	2.86
Cl	0.59
Ca	0.62
Mg	1.76
Al	4.49
Si	6.12
S	0.56
K	0.33
Fe	0.96
Zr	1.32

Fig. 9. SEM analysis of Pure PA202 resin after 1 year of operation. SEM photomicrographs of (A-B) resins morphology, (C—D) resins surface closeup, (E) elemental composition obtained from EDX spectrum. EDX spectrum is provided in supplementary materials as Fig. S5.

lower Cl content than the unused resin (0.59 % *vs.* 11.9 %). The Cl detected in the polymer sample may come from, *i.a*, the dissociated strongly basic amine functional groups present on the surface of the anion exchange resin in the form of $–R_4–N^+Cl^-$. The much lower concentration of Cl observed in the used sample may suggest ineffective regeneration of the resin bed, the functional groups of which have not been restored to their original chloride or hydrochloric form after sorption of NO_3^-, SO_4^{2-} and PO_4^{3-} ions. Another explanation could be that the additional contamination of the resin's surface may be so extensive that it led to a decrease in the percentage concentration of all the contained trace elements. This further confirmed that the surface of the resin was blocked. After a closer look at the installation interior, a similar problem was observed. Almost all filters, containers, and the inner part of the piping were overgrown with green-brown matter.

The installation was cleaned mechanically because no attempts at resin restoration using either non-oxidative or oxidative agents were successful, and the resin was replaced with a new batch. Subsequently, the efficiency of the technology was entirely restored. However, to avoid future problems related to increased eutrophication, an additional UV filter was placed in the water inlet before installation. Currently, this solution is being tested.

4. Conclusion

In this paper, the successful implementation of a water purification technology is presented. The idea focuses on the application of an installation consisting of ion exchange columns loaded into a container station that can operate directly in close proximity to the retention reservoir. On-site research allowed the optimisation of process parameters for the removal of NO_3^-, SO_4^{2-} and PO_4^{3-} reaching up to 97 % adsorption of NO_3^- over 100 m^3 of water passed through the installation. Although the applied resin was selective towards NO_3^-, the optimisation of the parameters allowed for the determination of the conditions and effectiveness for the removal of SO_4^{2-} and PO_4^{3-} as well.

The results confirmed the positive effect of technology on the quality of water flowing to the catchment area. A significant effect on the level of nitrogen compounds was observed in the case of the site factor. The concentrations of nitrogen compounds after treatment (Site_Outlet) were lower than before treatment (Site_Inlet). Additionally, treatment affected the oxygenation level (DO). Although the effect of water treatment on phosphorus compounds and BOD_5 was not demonstrated, the optimisation allowed us to conclude that a cascade design of the installation allows for the removal of PO_4^{3-}, and as such, satisfactory purification factors are expected.

The design of the technology allows to easily implement it at various sites, even those with limited access to the facilities. In this context,

based on the gained experiences, further works will involve altering composition and volume of regenerants, as their utilisation involved the main operation costs that the installation generated.

Funding

This research was funded by The National Centre for Research and Development (grant number BIOSTRATEG3/343733/15/NCBR/2018). The project leader was the University of Life Sciences in Wrocław. Piotr Cyganowski was supported by the Ministry of Education and Science (Poland) within the programme for outstanding young scientists.

CRediT authorship contribution statement

Piotr Cyganowski: Conceptualization (manuscript and process optimization), Formal analysis (process parameters), Methodology (process parameters), Supervision (process parameters), Visualization, Writing - original draft, Writing - review & editing. **Łukasz Gruss:** Conceptualization, Data curation (environmental studies), Formal analysis (environmental studies), Methodology (environmental studies), Resources, Software, Investigation (environmental studies), Visualization, Writing - original draft, Writing - review & editing. **Witold Skorulski** and **Tomasz Kabat**: Conceptualization (installation design), Investigation (process parameters), Project administration, Resources. **Paweł Piszko:** Investigation (infrared spectroscopy). **Dorota Jermakowicz-Bartkowiak:** Writing - review & editing. **Krzysztof Pulikowski:** Funding acquisition, Project administration, Supervision, Writing - review & editing. **Mirosław Wiatkowski:** Conceptualization, Validation, Funding acquisition, Project administration, Resources, Supervision, Writing - review & editing.

Declaration of competing interest

The authors declare no conflict of interests.

Data availability

The data that has been used is confidential.

Acknowledgements

The authors would like to express their sincere gratitude to the “Polish Waters” State Water Holding Regional Water Management Boards in Gliwice and the Catchment Management Board in Opole for assistance in the project. The authors wish to express their gratitude to Krystyna Woźniakowska, Joanna Szczypta, Kamila Hamal, Elżbieta Trośniak from the Environmental Research Laboratory of the UPWr and Michał Krawenda from the Electron Microscopy Laboratory of the UPWr for physicochemical analyses of water and SEM analysis.

References

[1] N. Bezak, M. Kovačević, G. Johnen, K. Lebar, V. Zupanc, A. Vidmar, S. Rusjan, Exploring options for flood risk management with special focus on retention reservoirs, Sustainability 13 (2021) 10099.
[2] S.W. Cooley, J.C. Ryan, L.C. Smith, Human alteration of global surface water storage variability, Nature 591 (2021) 78–81.
[3] D. Walker, D. Baumgartner, C. Gerba, K. Fitzsimmons, Surface water pollution, Environ. Pollut. Sci. (2019) 261–292.
[4] B. Grizzetti, O. Vigiak, A. Udias, A. Aloe, M. Zanni, F. Bouraoui, A. Pistocchi, C. Dorati, R. Friedland, A. De Roo, How EU policies could reduce nutrient pollution in European inland and coastal waters, Glob. Environ. Chang. 69 (2021) 102281.
[5] C. Grottera, C. Barbier, A. Sanches-Pereira, M.W. de Abreu, C. Uchôa, L. G. Tudeschini, J.-M. Cayla, F. Nadaud, A.O. Pereira Jr., C. Cohen, Linking electricity consumption of home appliances and standard of living: a comparison between Brazilian and French households, Renew. Sust. Energ. Rev. 94 (2018) 877–888.
[6] N.M. Pham, T.L.D. Huynh, M.A. Nasir, Environmental consequences of population, affluence and technological progress for European countries: a Malthusian view, J. Environ. Manag. 260 (2020) 110143.
[7] E. Fukase, W. Martin, Economic growth, convergence, and world food demand and supply, World Dev. 132 (2020) 104954.
[8] A. Srivastav, Chemical fertilizers and pesticides: role in groundwater contamination in agrochemicals detection, Treat. Remed. Butterworth-Heinemann (2020) 143–159.
[9] L.B. Owens, D.L. Karlen, Groundwater: nitrogen fertilizer contamination, managing water resources and hydrological systems, CRC Press (2020) 45–58.
[10] I. Rashmi, T. Roy, K. Kartika, R. Pal, V. Coumar, S. Kala, K. Shinoji, Organic and inorganic fertilizer contaminants in agriculture: impact on soil and water resources, Contamin. Agric. (2020) 3–41.
[11] A. Bandara, T. Akiyama, A Study on the Groundwater Contamination by the Agriculture Fertilizer Inputs and its Spatial Distribution Pattern in the Zhangye Basin, Northwest China, Bhumi, The Planning Research Journal, 2018, p. 6.
[12] T. Kondraju, K. Rajan, EXCESSIVE FERTILIZER USAGE DRIVES AGRICULTURE GROWTH BUT DEPLETES WATER QUALITY. ISPRS Annals of Photogrammetry, Remote Sensing & Spatial Information Sciences IV-3/W1, 2019, pp. 17–23.
[13] F. Serio, P.P. Miglietta, L. Lamastra, S. Ficocelli, F. Intini, F. De Leo, A. De Donno, Groundwater nitrate contamination and agricultural land use: a grey water footprint perspective in Southern Apulia Region (Italy), Sci. Total Environ. 645 (2018) 1425–1431.
[14] T. Addiscott, N. Benjamin, Nitrate and human health, Soil Use Manag. 20 (2004) 98–104.
[15] M.H. Ward, R.R. Jones, J.D. Brender, T.M. De Kok, P.J. Weyer, B.T. Nolan, C. M. Villanueva, S.G. Van Breda, Drinking water nitrate and human health: an updated review, Int. J. Environ. Res. Public Health 15 (2018) 1557.
[16] R. Gruca-Rokosz, M. Cieśla, Sediment methane production within eutrophic reservoirs: the importance of sedimenting organic matter, Sci. Total Environ. 799 (2021) 149219.
[17] D.M. Harper, Eutrophication of Freshwaters, Springer, 1992.
[18] Y. Li, J. Shang, C. Zhang, W. Zhang, L. Niu, L. Wang, H. Zhang, The role of freshwater eutrophication in greenhouse gas emissions: a review, Sci. Total Environ. 768 (2021) 144582.
[19] Y. Ontoria, E. Gonzalez-Guedes, N. Sanmarti, J. Bernardeau-Esteller, J.M. Ruiz, J. Romero, M. Perez, Interactive effects of global warming and eutrophication on a fast-growing Mediterranean seagrass, Mar. Environ. Res. 145 (2019) 27–38.
[20] M. Puchlik, J. Piekutin, K. Dyczewska, Analysis of the impact of climate change on surface water quality in north-eastern Poland, Energies 15 (2021) 164.
[21] A.K. Tiwari, D.B. Pal, Nutrients contamination and eutrophication in the river ecosystem, in: Ecological Significance of River Ecosystems, Elsevier, 2022, pp. 203–216.
[22] A. Bhatnagar, M. Sillanpää, A review of emerging adsorbents for nitrate removal from water, Chem. Eng. J. 168 (2011) 493–504.
[23] N. Öztürk, T.E.l. Bektaş, Nitrate removal from aqueous solution by adsorption onto various materials, J. Hazard. Mater. 112 (2004) 155–162.
[24] C. Lazaratou, D. Vayenas, D. Papoulis, The role of clays, clay minerals and clay-based materials for nitrate removal from water systems: a review, Appl. Clay Sci. 185 (2020) 105377.
[25] B. Wu, J. Wan, Y. Zhang, B. Pan, I.M. Lo, Selective phosphate removal from water and wastewater using sorption: process fundamentals and removal mechanisms, Environ. Sci. Technol. 54 (2019) 50–66.
[26] I.W. Almanassra, V. Kochkodan, G. Mckay, M.A. Atieh, T. Al-Ansari, Review of phosphate removal from water by carbonaceous sorbents, J. Environ. Manag. 287 (2021) 112245.
[27] R. Liu, L. Chi, X. Wang, Y. Sui, Y. Wang, H. Arandiyan, Review of metal (hydr)oxide and other adsorptive materials for phosphate removal from water, J. Environ. Chem. Eng. 6 (2018) 5269–5286.
[28] M.R. Awual, Efficient phosphate removal from water for controlling eutrophication using novel composite adsorbent, J. Clean. Prod. 228 (2019) 1311–1319.
[29] S. Al-Marri, S.S. AlQuzweeni, K.S. Hashim, R. AlKhaddar, P. Kot, R.S. AlKizwini, S. L. Zubaidi, Z.S. Al-Khafaji, Ultrasonic-Electrocoagulation Method for Nitrate Removal from Water, IOP Conf, Mater. Sci. Eng. IOP Publishing, Ser, 2020, p. 012073.
[30] K.S. Hashim, R. Al Khaddar, N. Jasim, A. Shaw, D. Phipps, P. Kot, M.O. Pedrola, A. W. Alattabi, M. Abdulredha, R. Alawsh, Electrocoagulation as a green technology for phosphate removal from river water, Sep. Purif. Technol. 210 (2019) 135–144.
[31] S.K. Huno, E.R. Rene, E.D. van Hullebusch, A.P. Annachhatre, Nitrate removal from groundwater: a review of natural and engineered processes, J. Water Supply Res. Technol. AQUA 67 (2018) 885–902.
[32] Y. Pang, J. Wang, Various electron donors for biological nitrate removal: a review, Sci. Total Environ. 794 (2021) 148699.
[33] L. Yan, C. Wang, J. Jiang, S. Liu, Y. Zheng, M. Yang, Y. Zhang, Nitrate removal by alkali-resistant Pseudomonas sp. XS-18 under aerobic conditions: performance and mechanism, Bioresour. Technol. 344 (2022) 126175.
[34] O. Pastushok, F. Zhao, D.L. Ramasamy, M. Sillanpää, Nitrate removal and recovery by capacitive deionization (CDI), Chem. Eng. J. 375 (2019) 121943.
[35] S.K. Sharma, R.C. Sobti, Nitrate removal from ground water: a review, E-J. Chem. 9 (2012) 1667–1675.
[36] D. Cliford, X. Liu, Ion exchange for nitrate removal, J. Am. Water Works Assoc. 85 (1993) 135–143.
[37] B. Buta, M. Wiatkowski, Ł. Gruss, P. Tomczyk, R. Kasperek, W. Skorulski, Wstępna analiza jakości wody zbiornika wodnego Turawa w obrębie działającej instalacji “WOPR”, Chem. Rev. 1 (2022) 52–60.
[38] A. Cygan, A. Kłos, P. Wieczorek, Using macroelement content to characterize surficial water quality of artificial reservoirs, Water Air Soil Pollut. 232 (2021) 1–15.

[39] Ł. Gruss, M. Wiatkowski, K. Pulikowski, A. Kłos, Determination of changes in the quality of surface water in the river—reservoir system, Sustainability 13 (2021) 3457.
[40] Z. Respondek, D. Jerz, P. Świsłowski, M. Rajfur, Active biomonitoring of heavy metal concentrations in aquatic environment using mosses and algae, Water 14 (2022) 3335.
[41] A. Steinhoff-Wrześniewska, M. Strzelczyk, M. Helis, A. Paszkiewicz-Jasińska, Ł. Gruss, K. Pulikowski, W. Skorulski, Identification of catchment areas with nitrogen pollution risk for lowland river water quality, Arch. Environ. Prot. 53-64-53-64 (2022).
[42] M. Wiatkowski, B. Wiatkowska, Changes in the flow and quality of water in the dam reservoir of the Mała Panew catchment (South Poland) characterized by multidimensional data analysis. Archives of, Environ. Prot. 45 (2019).
[43] R. Sadegh-Vaziri, M.U. Babler, Removal of hydrogen sulfide with metal oxides in packed bed reactors—a review from a modeling perspective with practical implications, Appl. Sci. 9 (2019) 5316.
[44] P. Cyganowski, Synthesis of adsorbents with anion exchange and chelating properties for separation and recovery of precious metals – a review, Solvent Extr. Ion Exch. (2020) 1–23.
[45] C. He, J. Huang, C. Yan, J. Liu, L. Deng, K. Huang, Adsorption behaviors of a novel carbonyl and hydroxyl groups modified hyper-cross-linked poly (styrene-co-divinylbenzene) resin for β-naphthol from aqueous solution, J. Hazard. Mater. 180 (2010) 634–639.
[46] S. Camli, S. Senel, A. Tuncel, Cibacron blue F3G-A-attached uniform and macroporous poly(styrene-co-divinylbenzene) particles for specific albumin adsorption, J. Biomater. Sci. Polym. Ed. 10 (1999) 875–889.
[47] J.L. Boudenne, S. Boussetta, C. Brach-Papa, C. Branger, A. Margaillan, F. Théraulaz, Modification of poly(styrene- co -divinylbenzene) resin by grafting on an aluminium selective ligand, Polym. Int. 51 (2002) 1050–1057.
[48] D.A. Long, Infrared and Raman Characteristic Group Frequencies, Tables and charts John Wiley & Sons, Ltd., Chichester, 2004.
[49] L.G. Wall, J.L. Tank, T.V. Royer, M.J. Bernot, Spatial and temporal variability in sediment denitrification within an agriculturally influenced reservoir, Biogeochemistry 76 (2005) 85–111.
[50] M.B. David, L.G. Wall, T.V. Royer, J.L. Tank, Denitrification and the nitrogen budget of a reservoir in an agricultural landscape, Ecol. Appl. 16 (2006) 2177–2190.
[51] A.J. Veraart, J.J. De Klein, M. Scheffer, Warming can boost denitrification disproportionately due to altered oxygen dynamics, PLoS One 6 (2011) e18508.
[52] T.L. Hamilton, J.R. Corman, J.R. Havig, Carbon and nitrogen recycling during cyanoHABs in dreissenid-invaded and non-invaded US midwestern lakes and reservoirs, Hydrobiologia 847 (2020) 939–965.
[53] C. Pompei, E. Alves, E.M. Vieira, L. Campos, Impact of meteorological variables on water quality parameters of a reservoir and ecological filtration system, Int. J. Environ. Sci. Technol. 17 (2020) 1387–1396.
[54] G. Chalar Marquisá, J.G. Tundisi, Main Processes in the Water Column Determined by Wind and Rainfall at Lobo (Broa) Reservoir: Implications for Phosphorus Cycling, 1999.
[55] L. Huang, H. Fang, G. He, H. Jiang, C. Wang, Effects of internal loading on phosphorus distribution in the Taihu Lake driven by wind waves and lake currents, Environ. Pollut. 219 (2016) 760–773.
[56] R. Jindal, M. Wats, Evaluation of surface water quality using water quality indices (WQIs) in Lake Sukhna, Chandigarh, India, Appl Water Sci 12 (2022) 1–14.
[57] C. Zhang, Q. Yan, N. Kuczyńska-Kippen, X. Gao, An Ensemble Kalman Filter approach to assess the effects of hydrological variability, water diversion, and meteorological forcing on the total phosphorus concentration in a shallow reservoir, Sci. Total Environ. 724 (2020) 138215.
[58] Accelerating Nutrient Pollution Reductions in the Nation''s Waters, Memorandum of United States Environmental Protection Agency, Washington, D.C. 20460, accessed online. https://www.epa.gov/system/files/documents/2022-04/accelerating-nutrient-reductions-4-2022.pdf, 2022.
[59] European Union, Directive 2000/60/EC (document no. 32000L0060), accessed online. https://eur-lex.europa.eu/legal-content/EN/TXT/?uri=celex%3A32000L0060, 2022.
[60] Nutrient Pollution, United States Environmental Protection Agency, Accessed online. https://www.epa.gov/nutrientpollution/sources-and-solutions-agriculture, 2022.
[61] Policy on nitrogen and phosphorus pollution, European Commision website, accessed online. https://ec.europa.eu/info/research-and-innovation/research-area/environment/nitrogen-and-phosphorus-pollution/policy_en, 2022.
[62] Regulation of the Minister of Infrastructure of June 25, 2021 on the classification of ecological status, ecological potential and chemical status, and the method of classification of the state of surface water bodies, as well as environmental quality standards for priority substances. webpage. 2022. https://leap.unep.org/en/countries/pl/national-legislation/regulation-classification-ecological-status-ecological-1.
[63] PA202 resin datasheet. Accessed online 2024. https://www.yumpu.com/en/document/view/1928490/pure-resin.
[64] W.J. Wolfgong, Chemical analysis techniques for failure analysis: Part 1, common instrumental methods." *Handbook of materials failure analysis with case studies from the aerospace and automotive industries*, Butterworth-Heinemann (2016) 279–307.